GeoStudio Example File
Effect of Climate on Groundwater Flow in a Hill Slope

To see the latest GeoStudio learning content, visit Seequent Learning Centre and search the catalogue for “GeoStudio”.

Seequent, The Bentley Subsurface Company

Introduction

Climate cycles can have a significant influence on groundwater recharge and flow patterns in hydrogeologic systems. The presence of pore-ice significantly reduces the hydraulic conductivity of the soil, effectively creating a confining layer that diminishes water transfer in some areas while diverting water in other areas. The thermal response of the system is governed not only by conductive heat transfer, but also by forced-convection (i.e. heat advection) with the moving of water. A TEMP/W analysis is used in this example to illustrate how seasonal air temperatures can change the regional groundwater flow patterns in a hill slope, where freezing air temperatures result in the recharge zone becoming cut off from the deeper flow system. This example is compared to results presented by McKenzie et al. (2007).

Background

The hill slope problem developed by McKenzie et al. (2007) considers recharge from a local topographic high to two nearby lakes with different surface elevations (Figure 1). The purpose of the model was to simulate groundwater flow during winter conditions, when freezing air temperatures restrict recharge to the system due to pore-ice formation in the frozen soil. The water in the lakes was assumed to be at a constant temperature, leading to a shift in the groundwater flow from the higher elevation lake to the lower elevation lake, until the air temperatures rise above freezing and the soil of the topographic high is thawed.

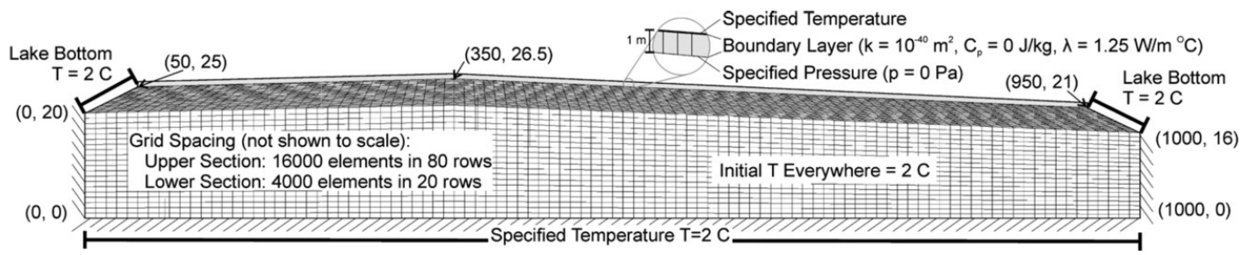

Figure 1. Problem configuration given in McKenzie et al. (2007).

Numerical Simulation

The configuration of the two-dimensional hill slope problem in GeoStudio is shown in Figure 2. The stratigraphy comprises a single aquifer unit overlain by a boundary layer. The boundary layer extends along the ground surface between the two lakes and was used to simulate the exchange of energy between the atmosphere and the soil surface. The boundary layer is used to buffer the temperature response at the ground surface, as it is well known the surface temperature does not equal the air temperature. It should be noted, however, that TEMP/W also includes a rigorous land-climate interaction boundary condition for computing the ground heat flux from a surface energy balance equation. The climate data requirements for land-climate interaction boundary condition, however, exceeded the data available in the case study. In order to compare with McKenzie et al. (2007), the surface layer was included in the analysis.

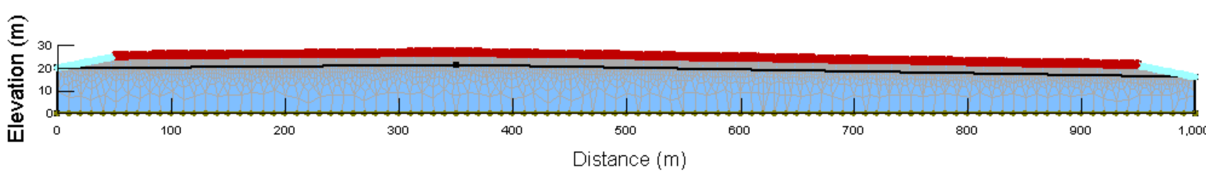

Figure 2. Problem configuration.

The Analysis Tree for the GeoStudio Project is shown in Figure 3. A steady-state SEEP/W analysis was used to establish the initial conditions for the transient forced-convection and water transfer analysis. It is important to give consideration to both conduction and forced-convection in this analysis because the recharge water will affect both the rate of freezing and thawing in the soil profile. It should also be noted that water transfer must be solved on the same domain in order for the temperature regime to impose an effect on water flow patterns (Figure 4). The initial conditions for the transient heat transfer analysis are established via a region activation temperature of 2°C.

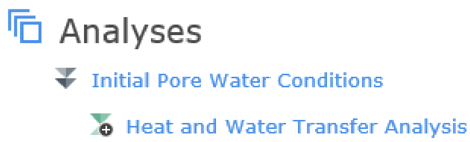

Figure 3 Analysis Tree for the GeoStudio Project

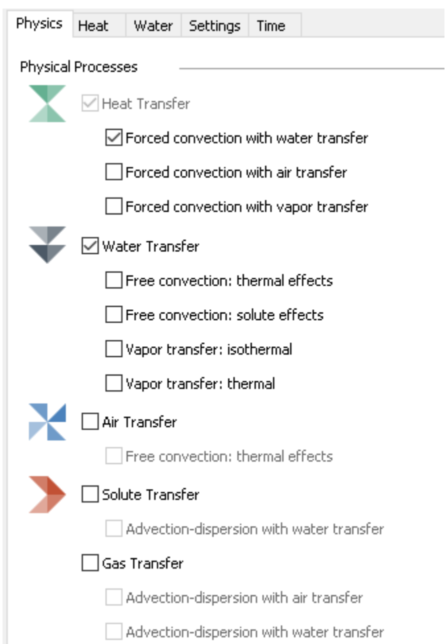

Figure 4. Physics tab for the forced-convection analysis.

The same hydraulic boundary conditions were used for the steady-state and transient water transfer analyses. A zero pore-water pressure condition was applied along the actual ground surface to ensure continuous infiltration into the domain. A constant total head boundary condition equal to the water elevation is applied to the right and left lakes.

The annual air temperature boundary condition was developed using a sinusoidal function with a 10° amplitude centered on an average annual temperature of 2°C (Figure 5). It is applied to the top of the boundary layer. Both lakes are assigned a constant temperature boundary condition of 2°C. McKenzie et al. (2007) also assumed an aquifer underlying the domain with a constant temperature of 2°C, so a constant temperature boundary condition was applied along the bottom of the model domain.

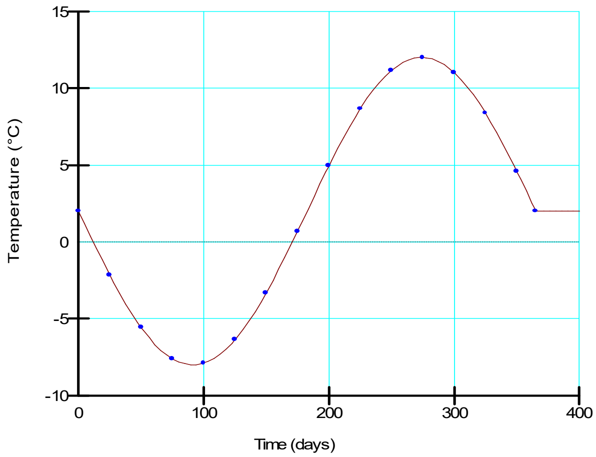

Figure 5. **Air temperature function.**

The hydraulic and thermal properties used in the analysis were based on McKenzie et al. (2007). The objective of this analysis is to match the patterns, not to replicate the exact values. As such, the GeoStudio estimation routines were used to develop the material property functions. The key inputs are listed in Table 1.

Table 1. Input variables for the calculated thermal material properties.

Thermal Property	Input variable
Specific Heat of Fluid	4182 J/kg/°C
Specific Heat of Ice	2108 J/kg/°C
Specific Heat of Solids	840 J/kg/°C
Thermal Conductivity of Fluid	0.6 J/sec/m/°C
Thermal Conductivity of Ice	2.14 J/sec/m/°C
Thermal Conductivity of Solids	3.5 J/sec/m/°C
Soil density	2600 kg/m^3
Ice density	920 J/kg
Water density	1000 kg/m^3
Porosity	0.1
S_{wres}	0.005

An unsaturated material model was used to define the hydraulic properties for the aquifer. The volumetric water content (VWC) function was estimated for sand with a saturated VWC of 0.1 and a coefficient of compressibility of 1 x 10^{-5} 1/kPa (Figure 6). The hydraulic conductivity function was estimated using a saturated hydraulic conductivity of 9.77 x 10^{-4} m/sec and a residual water content of 0.0005 (Figure 7). A hydraulic conductivity function is required in simulations where pore-ice blockage is expected to limit the flow of water, even if the domain is fully saturated. The Ky/Kx ratio was set to 0.01 to simulate the 1:100 anisotropic conditions described by McKenzie et al. (2007), with a minimum Kx of 9.77 x 10^{-10} m/sec. The boundary layer was defined using a saturated-only material model, with an arbitrarily low saturated hydraulic conductivity to minimize the amount of flow in this region.

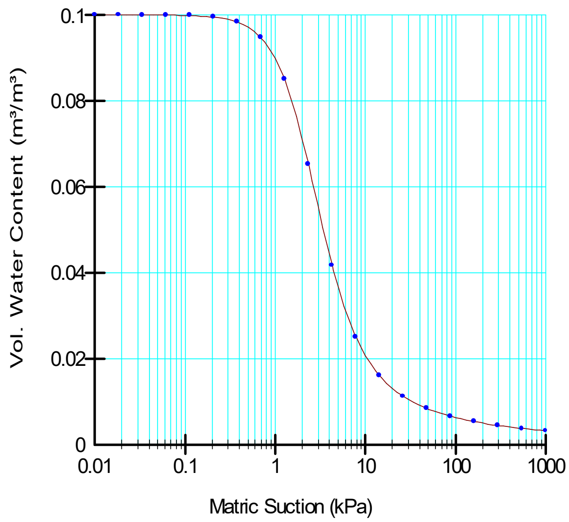

Figure 6. VWC function estimated using the Sand sample type in SEEP/W.

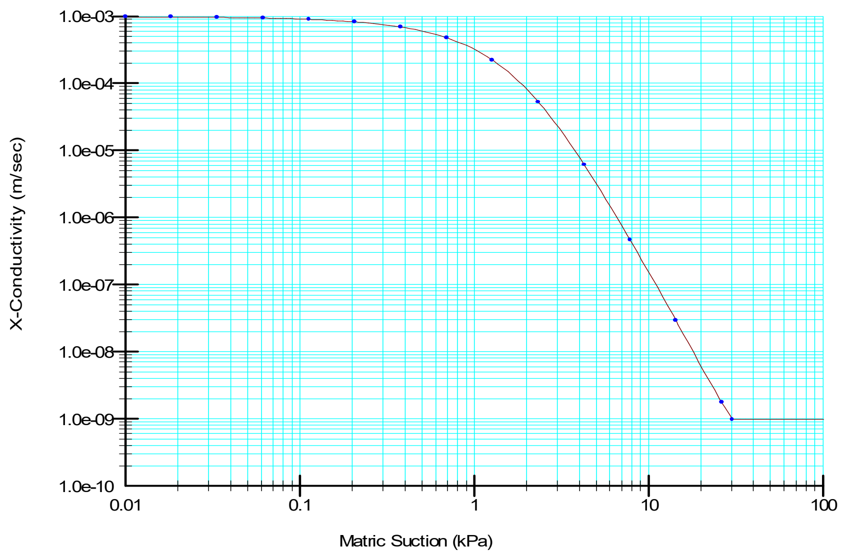

Figure 7. Hydraulic conductivity function.

The coupled convective thermal model was used to define the thermal material properties for the aquifer. Figure 8 presents the normalized unfrozen volumetric water content curve. The TEMP/W estimation functionality was used to define both the volumetric heat capacity and thermal conductivity functions, as shown in Figure 9 and Figure 10, respectively. Table 1 presents the key inputs taken from McKenzie et al., 2007. The boundary layer thermal conditions were defined using the simplified thermal material model, with a constant thermal conductivity of 1.25 J/sec/m/°C and a volumetric heat capacity of 0 kJ/m³/°C. The in situ water content was set to 0 to ensure that the boundary layer does not undergo phase change.

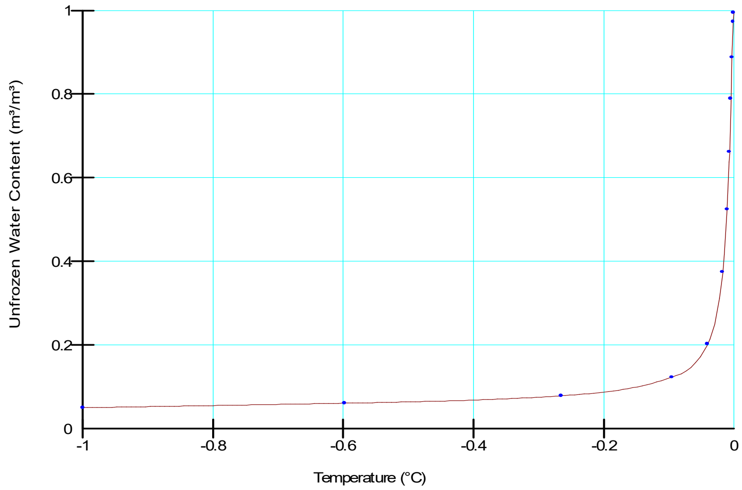

Figure 8. Unfrozen water content function.

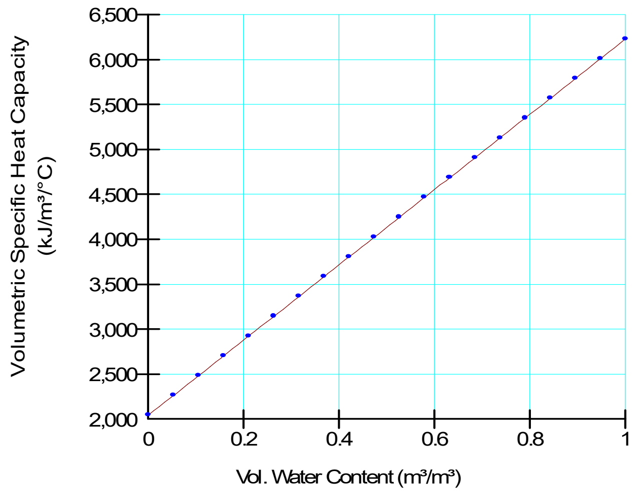

Figure 9. Volumetric specific heat capacity function.

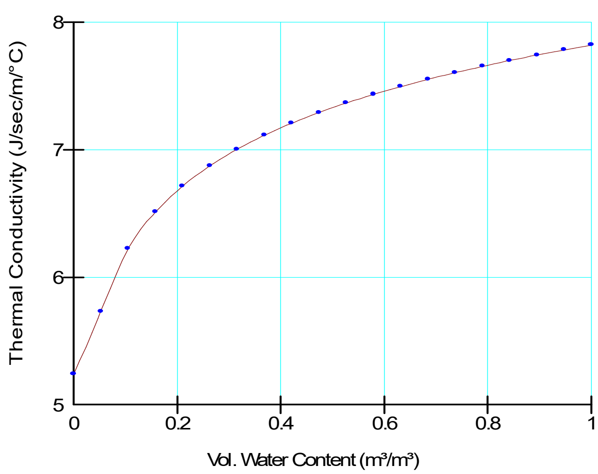

Figure 10. Thermal conductivity function.

Results and Discussion

The resulting surface temperatures along the hill slope were given by McKenzie et al. (2007) as shown in Figure 11. Figure 12 presents the corresponding TEMP/W results. The ground surface temperature response in TEMP/W reflects the same pattern and magnitudes as presented in the paper. Both analyses exhibit the zero curtain effect during freezing and thawing, which is indicated by the fairly flat portion of the temperature verses time plot. During this time, the perturbation of the freezing or thawing front stalls as sensible energy transferred to the phase boundary via conduction and forced-convection is converted into latent energy. The zero curtain effect is not as distinct in the Mckenzie et al. (2007) analysis due to the relaxed unfrozen water content function used in their analysis, in which the pore-water freezes over a temperature range of 0 to – 1°C. In contrast, TEMP/W uses a much steeper function (Figure 8).

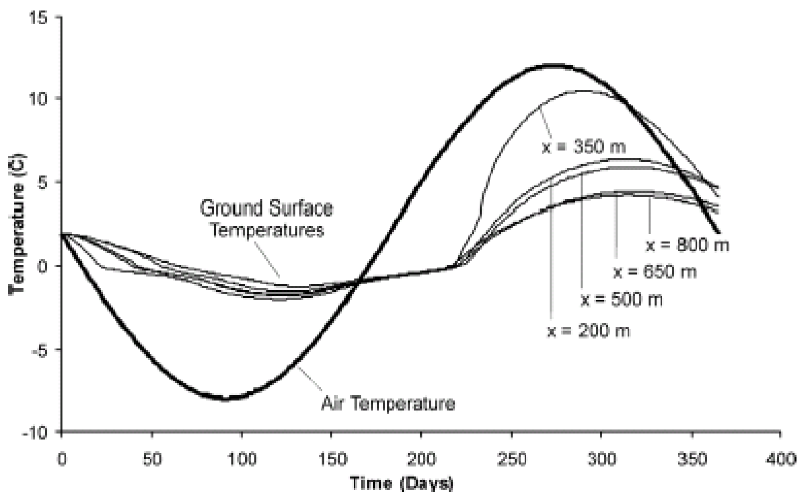

Figure 11. Surface temperature results reported by McKenzie et al. (2007).

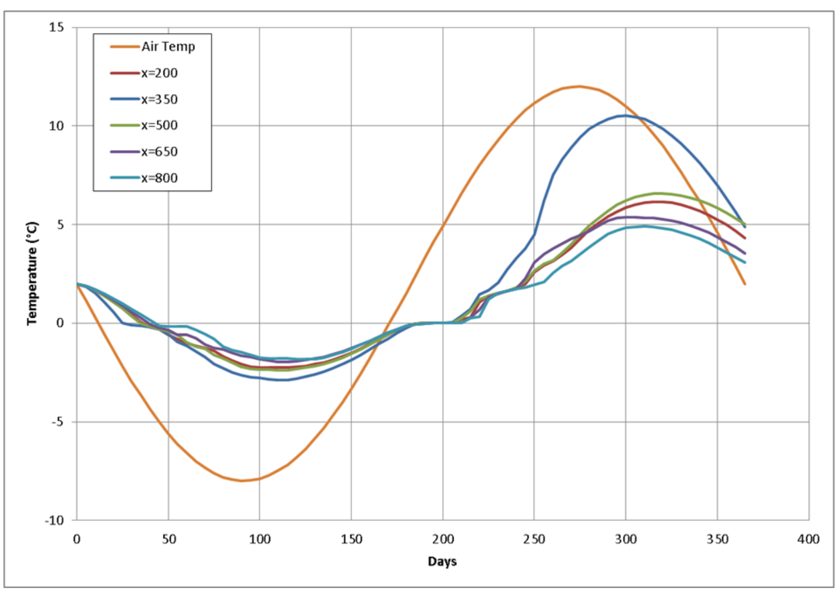

Figure 12. Surface temperature results using coupled convective model and internal TEMP/W functions.

Figure 13 presents the total head contours and flux vectors for the steady-state seepage analysis. The flux vectors are not perpendicular to the total head contours because of the large anisotropy ratio, which causes a tendency for horizontal flow. The phreatic surface drapes along the actual ground surface due to the zero pore-water pressure boundary condition. This naturally causes the maximum total head to be located at the topographic high, located at an x-coordinate of 350 m, and creates a groundwater divide at this location. Infiltration to the left of the divide flows towards the left lake, while the opposite happens on the right side.

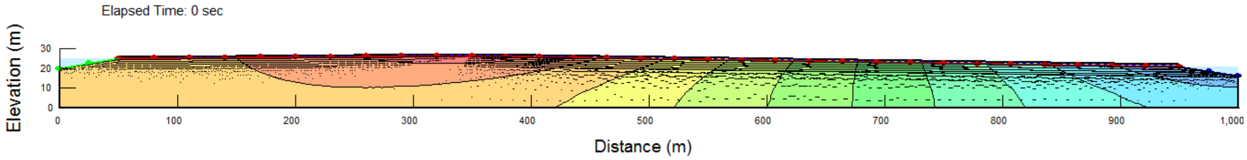

Figure 13. Flow pattern for steady-state conditions.

Figure 14 presents the water fluxes and location of the freezing front on Day 95, when the freezing front is almost at its maximum depth. Water flux occurs from the left lake at a total head of 25 m to the right lake (total head of 21 m). The hydraulic conductivity within the frozen zone is substantially reduced due to pore-ice blockage, effectively stopping downward infiltration. This causes a shift in the regional flow pattern as the total head contours change. Similar results were observed by McKenzie et al. (2007), where a shift in the regional flow pattern was observed on Day 90 (Figure 15). The maximum total head along the base of the aquifer (Figure 16) is at an x-coordinate of 350 m at the onset of the analysis. Once infiltration stops by Day 95, the total head distribution occurs from left-to-right with almost no flow in the frozen zone.

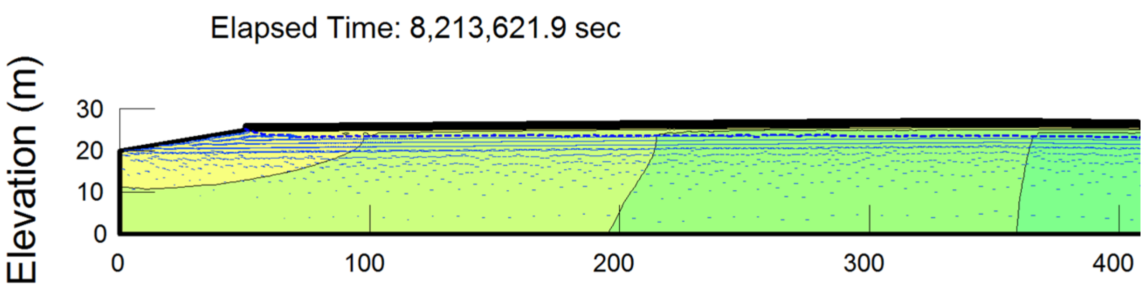

Figure 14. Water flux vectors and freezing front location on Day 95.

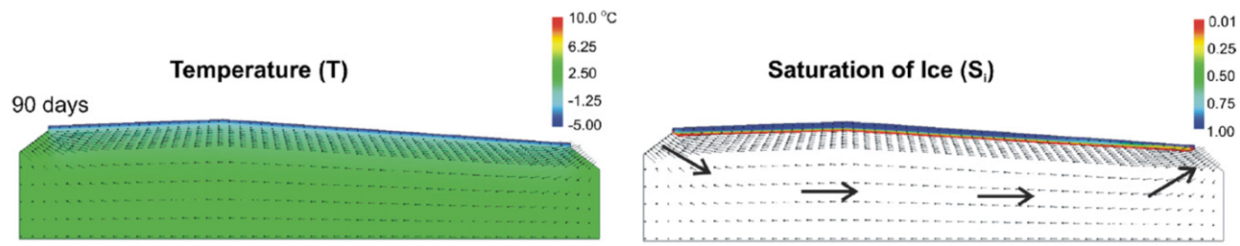

Figure 15. Temperature profiles, ice saturation and flow paths given by McKenzie et al. (2007) on Day 90.

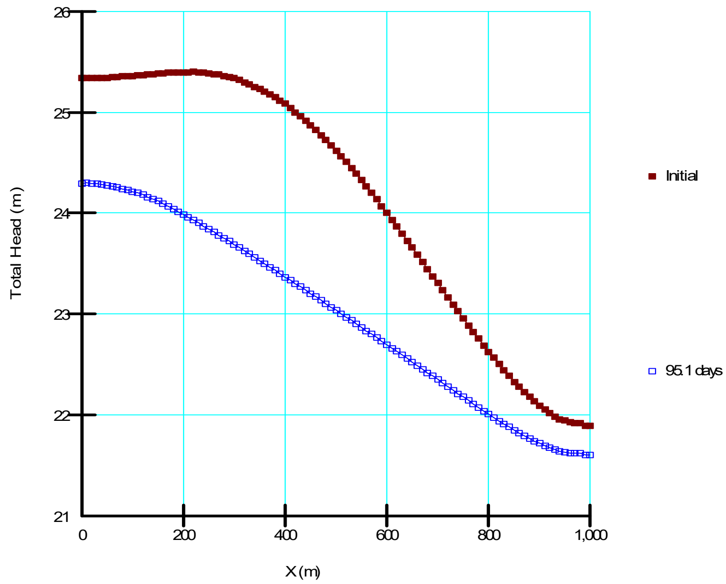

Figure 16. Total head along the base of the aquifer on Day 0 and Day 95.

Figure 17 presents the heat flux vectors on Day 95. It is interesting to note that heat flux is occurring almost entirely from left-to-right, in keeping with the water flow patterns, despite the fact that both lakes are at the same temperature. Heat transfer is dominated by forced-convection, which is driven by the water fluxes and not gradients in temperature. In contrast, heat transfer in the frozen zone is dominated by conduction because the water flux is negligible. The conductive heat flux is orders-of-magnitude lower than the forced-convection flux. As such, the heat flux vectors are not visible in the frozen zone at this scale.

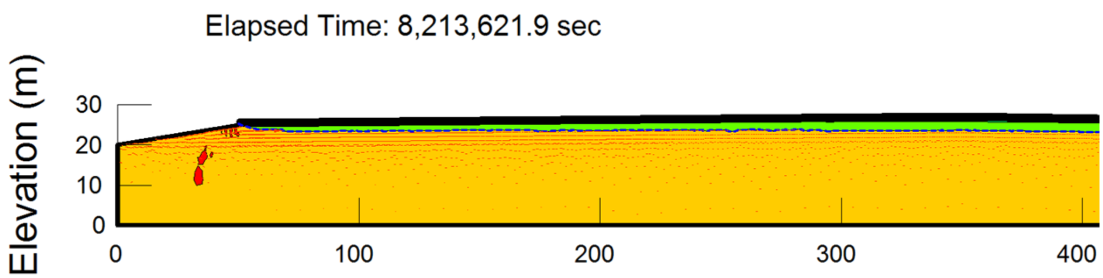

Figure 17. Heat fluxes and freezing front location on Day 95.

Ground thaw begins to occur in the spring as the ground surface temperature rises above freezing. The frost zone thaws due primarily to downward energy transfer from the ground surface and lateral transfer near the lakes. Figure 18 shows the flow pattern on day 220. Infiltration has resumed and water is moving laterally along the top of the low conductivity frozen zone. This ice zone continues to restrict deep percolation causing regional flow to continue from the left lake to the right lake. The advection of warm water into the system causes the frozen zone to disappear first at the hillcrest (Figure 19). At this point, the original regional flow pattern is restored. Similar patterns were observed by McKenzie et al. (2007), where the original flow system was return by Day 270 (Figure 20).

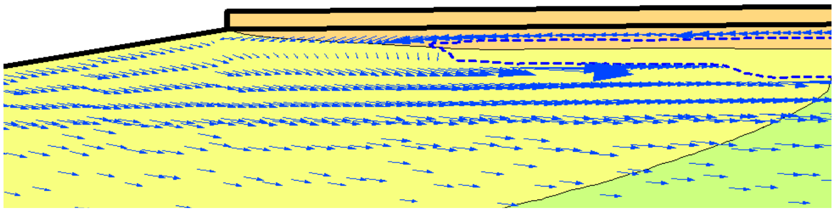

Figure 18. Flow pattern on Day 220.

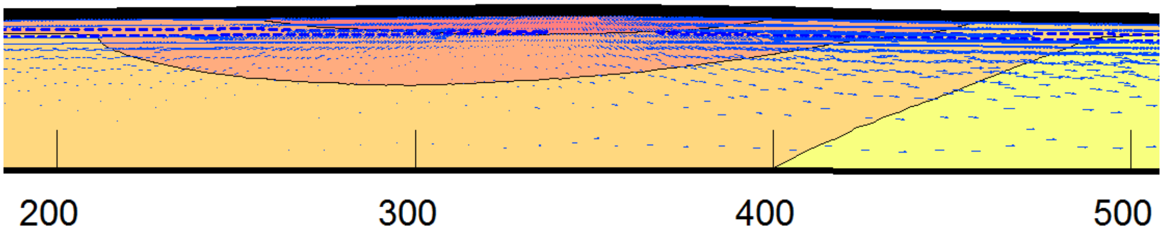

Figure 19. Extent of the frozen zone and flow pattern on Day 260, showing restoration of the regional flow system.

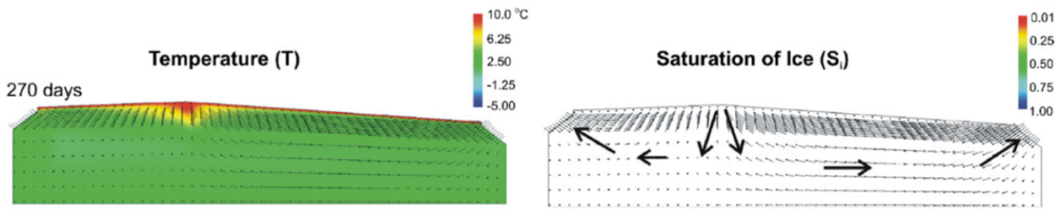

Figure 20. Temperature profiles, ice saturation and flow paths given by McKenzie et al. (2007) on Day 270.

Summary and Conclusions

A forced-convection TEMP/W analysis was used to explore the effect of climate on regional flow in a hill slope environment. The example was based on the benchmark example proposed by McKenzie et al., 2007. The numerical analysis revealed the significant role of ground freezing on infiltration and flow patterns. Infiltration ceased as the frozen zone propagates downward and the hydraulic of the soil was reduced due to pore-ice blockage. In turn, the total head contours were altered and regional flow patterns changed. The original flow system was restored once the frozen zone disappeared near the hillcrest.

References

Domenico, P.A. and Schwartz, F.W. 1990. Physical and Chemical Hydrogeology. John Wiley & Sons, Inc., New York, NY.

McKenzie, J.M., Voss, C.I. and Siegel, D.I. 2007. Groundwater flow with energy transport and water-ice phase change: numerical simulations, benchmarks, and application to freezing in peat bogs. Advances in Water Resources, 30, 966-983. Elsevier Ltd.